SCOUR PREDICTION AT SRISAILAM DAM (INDIA)

E.F.R. Bollaert, AquaVision Engineering, Switzerland

Abstract

This paper presents a comprehensive evaluation of 20 years of plunge pool scour development at Srisailam Dam, Andhra Pradesh, India. A new physically-based engineering model estimating scour formation as a function of time, the Comprehensive Scour Model (CSM), is used for this purpose.

The basic premises of this model have been extensively described in Bollaert (2002, 2004) and Bollaert & Schleiss (2005). The model allows estimating the time evolution of scour by describing turbulent jet diffusion through a plunge pool and accounting for specific geomechanic characteristics of the fractured bedrock. At Srisailam Dam, detailed data on bathymetric surveys and gate operations since 1984 allowed sound calibration of the model and, thus, a reasonable prediction of future potential scour formation during the design flood event.

Keywords: scour prediction, comprehensive scour model, fractured rock, design flood event

1. Introduction

Scour of rock due to high-velocity jets has been of concern to practicing engineers for a long time. Today's most popular evaluation methods are mostly of empirical and semi-empirical character. They do not entirely describe the physics behind the phenomenon. Therefore, a new model has been developed, based on a detailed parametric description of the main physical processes that are responsible for scour (Figure 3). The basic premises of this model have been extensively described in Bollaert (2002, 2004) and Bollaert & Schleiss (2005). The model allows estimating the time evolution of scour by accounting for turbulent jet diffusion through a plunge pool and the specific geomechanic characteristics of the fractured bedrock.

2. Background and data

Srisailam Dam is situated across the river Krishna, in the Kurnool District of Andhra Pradesh, India. It is about 110 km upstream of Nagarjunasagar dam and about 200 km from Hyderabad. The project consists of a 143 m high masonry dam and a right bank power station equipped with 7 units of 110 MW each. The power station is located about 450 m downstream of the dam. The dam reservoir has a full storage level of 269.75 m a.s.l. for a capacity of 8'720 million m^3. The dam spillway has been provided in the deep river portion with non-overflow blocks on either side. The spillway has an overall operating crest length of 266.4 m at en elevation of 252.98 m a.s.l. It comprises 12 spans of 18.30 m clear width, equipped with radial crest gates of 18.30 x 21.49 m, as shown in Figure 1.

The maximum design discharge is of 38'370 m^3 at a maximum reservoir level of 271.88 m a.s.l. A ski-jump bucket with invert at 188.98 m a.s.l. has been provided for energy dissipation at the downstream toe of the dam. Two sluices provided in the right flank non-overflow portion are designed to pass a maximum discharge of 1'500 m^3.

Dam construction started in 1963 and was completed in 1984 including erection of the spillway gates. During construction, deep scour was observed near the toe of the dam. The toe was protected from undermining by the progressive construction of a 36 m wide concrete apron in front of blocks N° 8 to 18 (Fig. 1) between 1977 and 1981. During subsequent years undermining of the concrete apron persisted and necessary measures were taken for protection. Due to concern about intensive spray affecting the power station and complex and the roads along the banks, the end spans of the spillway have never been operated for flood relief.

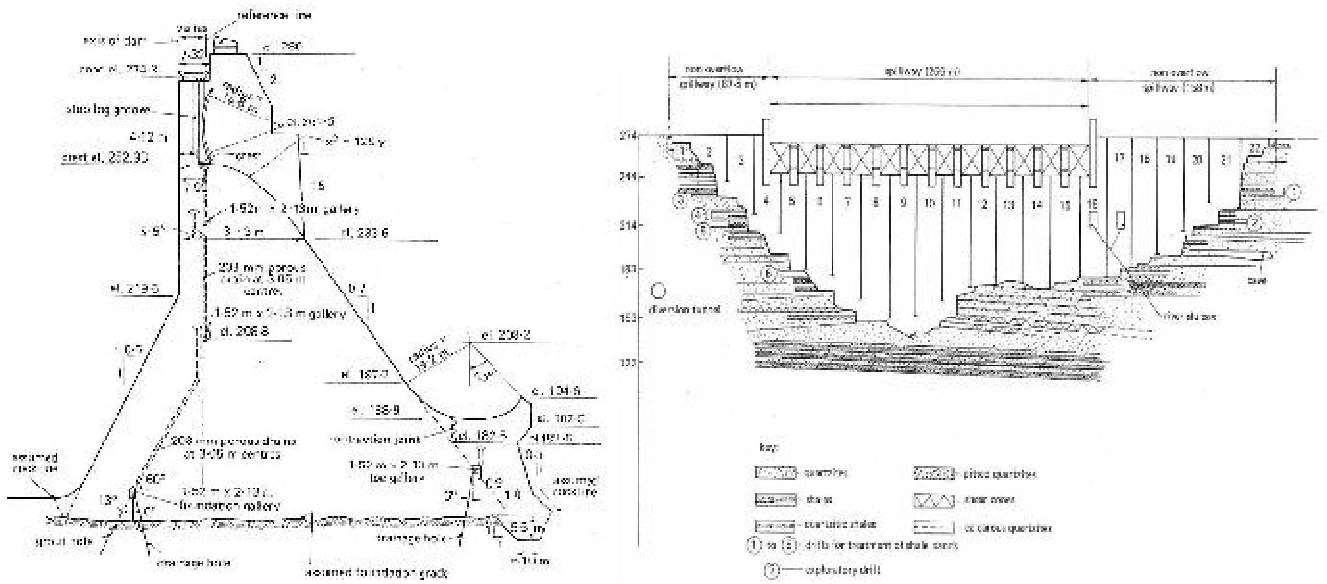

a) b)

Figure 1: a) Cross-section at Srisailam Dam; b) Rock layers at the dam site (Swamy, 1979).

Swamy (1979) stated that the bedrock at the dam site is associated with many joints, intercalations of soft shales, weak pockets, sheared and fractured zones, cavities and so on. He highlighted the presence of horizontally disposed shear zones between 145 and 154 m a.s.l. as presented in Figure 1b.

The history of scour formation is presented in Figure 2 (Mason, 2000). Three flood events were responsible for major scour progression: the 1986 (9'000 m^3/s), 1988 (12'000 m^3/s) and 1998 (24'000 m^3/s) floods.

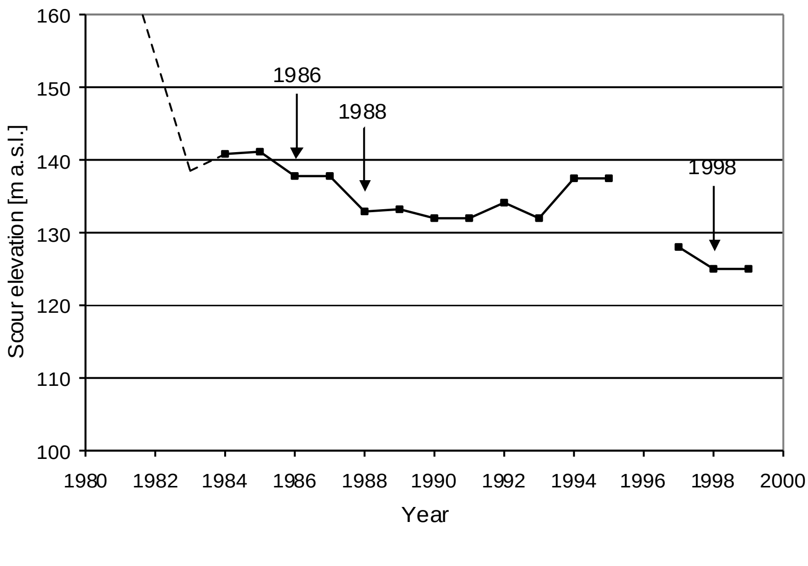

Figure 2: History of scour progression at Srisailam Dam (Mason, 2000)

3. Comprehensive Scour Model (Bollaert, 2002 and 2004)

The Comprehensive Scour Model has been developed based on experimental and numerical investigations of dynamic water pressures in rock joints (Bollaert, 2002). The model comprises two methods that describe failure of jointed rock. The first one, the *Comprehensive Fracture Mechanics* (CFM) method, determines the ultimate scour depth by expressing instantaneous or time-dependent joint propagation due to water pressures inside the joint. The second one, the *Dynamic Impulsion* (DI) method, describes the ejection of rock blocks from their mass due to sudden uplift pressures. The structure of the Comprehensive Scour Model consists of three modules: the falling jet, the plunge pool and the rock mass. The latter module implements the two aforementioned failure criteria. More details on the model equations can be found in Bollaert (2004) and Bollaert & Schleiss (2005).

3.1 The module of the falling jet

This module describes how the hydraulic and geometric characteristics of the jet are transformed from dam issuance down to the plunge pool (Fig. 3). Three parameters characterize the jet at issuance: the velocity V_i, the diameter (or width) D_i and the initial turbulence intensity Tu, defined as the ratio of velocity fluctuations to the mean velocity (2). The jet trajectory is based on ballistics and air drag and will not be further outlined. The jet module computes the longitudinal location of impact, the total trajectory length L and the velocity and diameter at impact V_j and D_j.

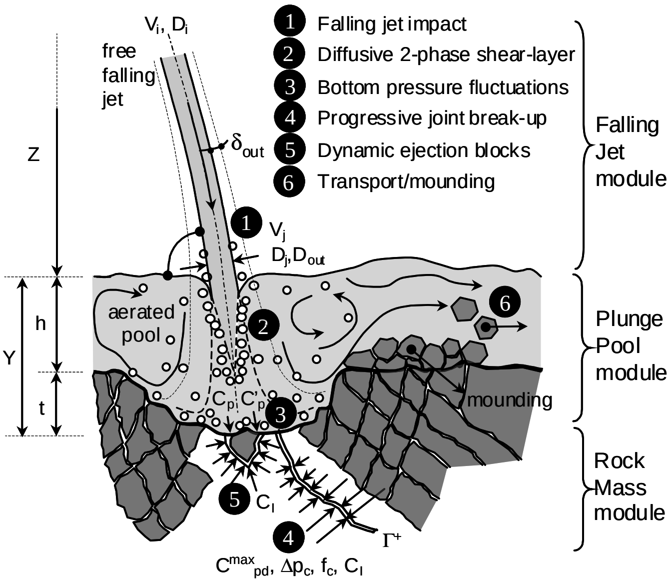

Figure 3: Main physical-mechanical processes responsible for rock scour (Bollaert, 2004)

3.2 The module of the plunge pool

This module describes the characteristics of the jet when traversing the plunge pool defining so the water pressures at the water-rock interface. The plunge pool water depth Y is essential. For near-vertically impacting jets, it is defined as the difference between the water level and the bedrock level at the point of impact. The water depth increases with discharge and scour formation. Initially, Y equals the tailwater depth t (Fig. 3). During scour formation, Y has to be increased with the depth of the formed scour h. The water depth Y and jet diameter at impact D_j determine the ratio of water depth to jet diameter at impact Y/D_j. This ratio is directly related to jet diffusion.

The most relevant pressures are the mean dynamic pressure coefficient C_{pa} and the root-mean-square (rms) coefficient of the fluctuating dynamic pressures C'_{pa}, both measured directly under the centerline of the jet. These coefficients correspond to the ratio of pressure head (in [m]) to incoming kinetic energy of the jet ($V^2/2g$) and are defined in Bollaert (2004).

3.3 The module of the rock mass

The pressures defined at the bottom of the pool are used for determination of the transient pressures inside open-end or closed-end rock joints. The parameters are:

1. maximum dynamic pressure coefficient C^{max}_{p}
2. characteristic amplitude of pressure cycles Δp_c
3. characteristic frequency of pressure cycles f_c
4. maximum dynamic impulsion coefficient C^{max}_{I}

The first parameter is relevant to brittle propagation of closed-end rock joints. The second and third parameters express time-dependent propagation of closed-end rock joints. The fourth parameter is used to define dynamic uplift of rock blocks formed by open-end rock joints.

The maximum dynamic pressure C^{max}_p is obtained through multiplication of the rms pressure C'_{pa} with an amplification factor Γ^+, and by superposition with the mean dynamic pressure C_{pa}. Γ^+ expresses the ratio of the peak value inside the rock joint to the rms value of pressures at the pool bottom and has been determined based on prototype-scaled experiments (Bollaert, 2004). The product of C'_{pa} times Γ^+ results in a maximum pressure, written as:

$$P_{\max}[Pa] = \gamma \cdot C_p^{\max} \cdot \frac{V_j^2}{2g} = \gamma \cdot \left(C_{pa} + \Gamma^+ \cdot C'_{pa}\right) \cdot \frac{V_j^2}{2g} \qquad (2)$$

As the experiments were performed for both stable and unstable (broken up) jets, the degree of break-up is automatically accounted for in the definition of the C_{pa} and C'_{pa} parameters.

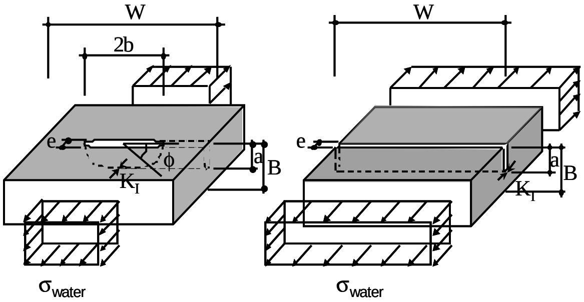

Figure 4: Main types of rock joints used in the Comprehensive Fracture Mechanics model (Bollaert, 2004)

The main uncertainty of Eq. (2) lies in the Γ^+ factor. It is interesting to notice that, based on Eq.(2), maximum pressures inside joints occur for Y/D_j ratios between 8 and 10. This means that the most critical flood situation may not be the PMF but rather the flow that results in a critical Y/D_j ratio.

The characteristic amplitude of the pressure cycles, Δp_c, is determined by the maximum and minimum pressures of the cycles. The characteristic frequency of pressure cycles f_c follows the assumption of a perfect resonator system and depends on the air concentration in the joint α_i and on the joint length L_f.

Beside the dynamic pressure inside rock joints, the resistance of the rock has to be determined. The cyclic character of the pressures generated by the impact of a high-velocity jet makes it possible to describe joint propagation by fatigue stresses occurring at the tip of the joint. This can be described by Linear Elastic Fracture Mechanics (LEFM). A simplified methodology is used (Bollaert, 2004). The method attempts to describe the main principles such that engineering applications become plausible. It is called the Comprehensive Fracture Mechanics (CFM) method and applicable to any partially jointed rock. Pure tensile pressure loading inside rock joints is described by the stress intensity factor K_I. This parameter represents the amplitude of the rock mass stresses that are generated by the water pressures at the tip of the joint. The corresponding resistance of the rock mass against joint propagation is expressed by its fracture toughness K_{Ic}.

The issue is to obtain a comprehensive and physically correct implementation of the complex and dynamic situation encountered in fractured rock. Joint propagation distinguishes between *brittle* (or instantaneous) joint propagation and *time-dependent* joint propagation. The former happens for a stress intensity factor that is equal to or higher than the fracture toughness of the material. The latter is occurring when the maximum possible water pressure results in a stress intensity that is inferior to the material's resistance. Joints may then be propagated by fatigue. Failure by fatigue depends on the frequency and the amplitude of the load cycles. The fracture mechanics implementation of the hydrodynamic loading consists of a transformation of the water pressures in the joints into stresses in the rock. These stresses are characterized by K_I as follows:

$$K_I = P_{\max} \cdot F \cdot \sqrt{\pi \cdot L_f} \qquad (3)$$

in which K_I is in MPa$\sqrt{m}$ and P_{max} (eq. 2) in MPa.

The boundary correction factor F depends on the type of crack and on its persistency, i.e. its degree of cracking defined as a/B or b/W in Fig. 4. This figure presents two basic configurations for partially jointed rock. The choice of the most relevant geometry depends on the type and the degree of jointing of the rock.The first crack is of semi-elliptical shape and partially sustained by the surrounding rock mass in two horizontal directions. Corresponding stress intensity factors should be used in case of low to moderately jointed rock. The second crack is single-edge notched and of two-dimensional nature. Support from the surrounding rock mass is only exerted perpendicular to the plane of the notch and, as a result, stress intensity factors will be substantially higher. Thus, it is appropriate for significantly to highly jointed rock.

For practice, F values of 0.5 or higher are considered to correspond to completely broken-up rock, i.e. the DI method becomes more applicable than the CFM method. For values of 0.1 or less, a tensile strength approach is more plausible. However, most of the values in practice are between 0.20 and 0.40, depending on the type and number of joint sets, the degree of weathering, joint interdistances, etc.

The fracture toughness K_{Ic} has been related to the mineralogical type of rock and to the unconfined compressive strength UCS. Furthermore, corrections are made to account for the loading rate and the in-situ stress field. The corrected fracture toughness is defined as the in-situ fracture toughness $K_{I,ins}$ and is based on a linear regression of available literature data. More detailed equations, as a function of the mineralogical rock composition, can be found in Bollaert (2002).

$$K_{I\ ins,\ UCS} = (0.008 \text{ to } 0.010) \bullet UCS + (0.054 \bullet \sigma_c) + 0.42 \qquad (4)$$

in which σ_c represents the confinement horizontal in-situ stress and T, UCS and σ_c are in MPa. Instantaneous joint propagation will occur when $K_I > K_{Iins}$. If not, joint propagation needs a certain time to happen. This is expressed by an equation as originally proposed to describe fatigue growth in metals:

$$\frac{dL_f}{dN} = C_r \cdot \left(\Delta K_I / K_{Ic}\right)^{m_r} \qquad (5)$$

in which N is the number of pressure cycles. C_r and m_r are material parameters that are determined by fatigue tests and ΔK_I is the difference of maximum and minimum stress intensity factors. To implement time-dependent joint propagation into the model, m_r and C_r have to be known. They represent the vulnerability of rock to fatigue and can be derived from available literature data on quasi-steady break-up by water pressures in joints (Atkinson, 1987). A first-hand calibration for granite (Cahora-Bassa Dam; Bollaert, 2002) resulted in C_r = 1E-8 for m_r = 10.

The fourth dynamic loading parameter is the maximum dynamic impulsion C^{max}_I in an open-end rock joint (underneath a single rock block), obtained by time integration of the net forces on the block (Newton):

$$I = \int_0^{\Delta tpulse} \left(F_u - F_o - G_b - F_{sh}\right) \cdot dt = m \cdot V_{\Delta tpulse} \qquad (6)$$

in which F_u and F_o are the forces under and over the block, G_b is the immerged weight of the block and F_{sh} represents the shear and interlocking forces. The shape of a block and the type of rock define the immerged weight. Shear and interlocking forces depend on the joint pattern and the in-situ stresses. As a first approach, they can be neglected. The pressure field over the block is governed by jet diffusion. The pressure field under the block corresponds to transient pressure waves.

The first step is to define the maximum net impulsion I_{max}. I_{max} is defined as the product of a net force and a time period. The corresponding pressure is made non-dimensional by the jet's kinetic energy $V^2/2g$. This results in a net uplift pressure coefficient C_{up}. The time period is non-dimensionalized by the travel period that is characteristic for pressure waves inside rock joints, i.e. $T = 2 \cdot Lf/c$. This results in a time coefficient T_{up}. Hence, the non-dimensional impulsion coefficient C_I is defined by the product $C_{up} \cdot T_{up} = V^2 \cdot L/g \cdot c$ [m·s]. The maximum net impulsion I_{max} is obtained by multiplication of C_I by $V^2 \cdot L/g \cdot c$. Prototype-scaled analysis of uplift pressures resulted in the following expression for C_I:

$$C_I = 0.0035 \cdot \left(\frac{Y}{D_j}\right)^2 - 0.119 \cdot \left(\frac{Y}{D_j}\right) + 1.22 \qquad (7)$$

Failure of a block is expressed by the displacement it undergoes due to the net impulsion C_I. This is obtained by transformation of $V_{\Delta tpulse}$ in Eq. (6) into a net uplift displacement h_{up}. The net uplift displacement that is necessary to eject a rock block from its matrix is difficult to define. It depends on the protrusion and the degree of interlocking of the blocks. A first-hand calibration on Cahora-Bassa Dam (Bollaert, 2002) resulted in a critical net uplift displacement of 0.20.

4. Scour at Srisailam Dam

The Comprehensive Scour Model (CSM) has been applied to the Srisailam Dam scour formation. First, the model has been calibrated based on 20 years of in-situ measured scour. Next, the model has been applied to design flood conditions to predict potential further scour progression.

4.1 Jet and plunge pool

Figure 5 presents the jet trajectory and the plunge pool geometry for a unit flow discharge of about 50 m^3/s/m. The flow characteristics on the spillway chute have been computed from the dam crest to the lip of the flip bucket by means of a 1D two-phase numerical model for steep slopes. This allowed defining the thickness and velocity of the jet at the bucket lip for different unit flows.

It can be noticed that the jet has a very flat rectangular shape, for a width-to-depth ratio between 5 and 18, with an average value of about 9. As such, the jet issuing from the bucket lip will most probably not completely transform into a quasi-circular shape but rather stay rectangular. Next, based on the available data on gate operations and unit flows, an average unit flow of 62 m^3/s/m and average head-and tailwater levels of 268 and 180 m a.s.l. have been defined. Based on these values, the main parameters of the falling jet and plunge pool modules have been computed. They are summarized at Table 1a.

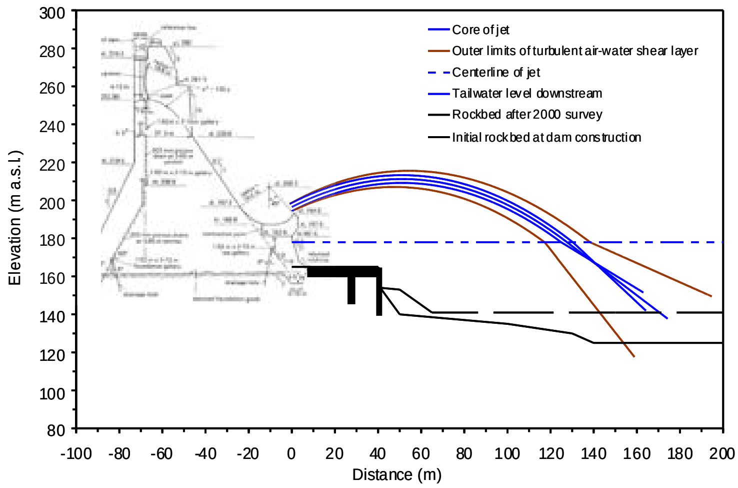

Figure 5: Trajectory of falling jet for a unitary discharge of 50 m^2/s

Jet Issuance from flip bucket of spillway chute			
Unit discharge	q	m^2/s	62.0
Total discharge	Q	m^3/s	13600
Issuance velocity	V_i	m/s	34.0
Issuance width	b_i	m	18.3
Issuance equivalent diameter	D_i	m	6.7
Angle	θ_i	°	45
Turbulence intensity	Tu_i	%	4
Jet impact in plunge pool			
Velocity	V_j	m/s	39.0
Core diameter	D_j	m	3.6
Outer diameter	D_{out}	m	13.8
Angle of jet	θ_j	°	-40.7
Distance from dam toe	x_{ult}	m	120
Air drag reduction	K	-	0.9
Trajectory length	L_j	m	128
Break-up length	L_b	m	60
Degree of break-up	L_b/L_j	-	2.13
Jet impact at rock bed			
Initial water depth	Y	m	38
Static pressure	Cstat	-	0.52
Mean dynamic pressure	Cpa	-	0.10
RMS dynamic pressure	C'pa	-	0.11
Amplification factor	Γ^+	-	4

a)

	Property	Symbol	AVERAGE	Unity
Quartzite	Unconfined Compressive Strength	UCS	130	MPa
	Density rock	γ_r	2700	kg/m3
	Ratio horizontal/vertical stresses	K_0	1	-
	Typical maximum joint length	L	1	m
	Vertical persistence of joint	P	0.35	-
	Form of rock joint	-	elliptical	-
	Tightness of joints	-	tight	-
	Total number of joint sets	N_j	4	-
	Typical rock block length	l_b	1	m
	Typical rock block width	b_b	1	m
	Typical rock block height	z_b	0.75	m
	Joint wave celerity	c	150	m/s
	Fatigue sensibility	m	9	-
	Fatigue coefficient	C	1.00E-07	-
Shale	Unconfined Compressive Strength	UCS	40	MPa
	Density rock	γ_r	2400	kg/m3
	Ratio horizontal/vertical stresses	K_0	1	-
	Typical maximum joint length	L	1	m
	Vertical persistence of joint	P	0.35	-
	Form of rock joint	-	elliptical	-
	Tightness of joints	-	tight	-
	Total number of joint sets	N_j	4	-
	Typical rock block length	l_b	0.1	m
	Typical rock block width	b_b	0.1	m
	Typical rock block height	z_b	0.050	m
	Joint wave celerity	c	125	m/s
	Fatigue sensibility	m	5	-
	Fatigue coefficient	C	2.00E-07	-

b)

Table 1: a) Jet and plunge pool parameters; b) Average rock mass parameters

4.2 Rock mass

The main rock mass characteristics are summarized at Table 1b. Based on Swamy (1979) and Mason (2000), the bedrock is considered to be a mixture of quartzite and shales. As presented in Figure 2, two distinct rock layers are distinguished at the site, quartzite and shale, with different characteristics. Quartzite is located near the surface, while near-horizontal plane shale intercalations are present under the form of 0.2 to 0.9 m bands between the crushed quartzite at elevations of 130 m a.s.l. and deeper. No direct information could be obtained related to the UCS strength of the intact rock at the site. However, based on Bollaert (2002), the UCS strengths of quartzite are directly related to their fracture toughness K_{Ic}. Based on typical K_{Ic} values available in literature for quartzites between 2 and 2.5, high UCS values of 210-270 MPa are obtained. These values are not site-specific although.

Gowda et al. (1999) performed a seismic survey of the plunge pool and determined the seismic wave velocity of the quartzite bedrock at Srisailam between 4000 and 5500 m/s, indicating a basically non-weathered rock. Use of the above seismic velocities results in K_{Ic} values between 0.9 and 1.8 MPa$\sqrt{}$m, or UCS values between 80 and 180 MPa.

Hence, in the following, this range of values has been used as input to the CSM model. The lower bound represents a conservative value, while the upper bound represents a beneficial assumption. An average UCS value is defined at 130 MPa. The main average parametric values are defined at Table 1b. The fatigue parameters of the rock layers, as well as other parameters of Table 1b, have been chosen based on previous calibrations made for granite at Cahora-Bassa Dam (Bollaert and Schleiss, 2005) and at Kariba Dam (Bollaert, 2005).

The CSM scour computations have been performed for the quartzite rock layer. A more complete analysis would need additional computations accounting for both shale and quartzite layers.

4.3 Results of CSM computations

Figures 6a to 6d present the scour evolution as a function of the duration of flood spillage. The times of flood duration between 1984 and 1998 have been computed as an average of the four most used gates. As such, since 1984, the spillway has been functioning on the average for about 12'000 hours. Both the Fracture Mechanics (CFM) and the Dynamic Impulsion (DI) methods have been applied. The former provides scour formation as a function of flood duration, while the latter only provides an ultimate state of scour formation.

Figure 6a presents the computational results for an average unit flow of 62 m^3/s/m, or total flow of about 13'500 m^3/s. This flow is more or less representative for almost all years of flooding between 1984 and 1998, except the year 1998, for which a unit flow of 110 m^3/s has been noticed. Based on Gowda et al. (1999), the initial bedrock at the point of impact of the jet, i.e. about 160 m downstream of the dam toe, is situated around 135 m a.s.l. Hence, this level has been used as initial level for the computations. It can be seen on Figure 6a that no scour is computed by both models, which seems to agree fairly well with the prototype observations. Gowda et al. (1999) concluded that no significant scour could be observed in the middle of the plunge pool. Only along the left bank, local scour of 2-4 m deep has formed.

Second, the 1998 event produced about 10 m of scour in the middle of the plunge pool. This is mainly because this event has a unit flow of about twice the average of the previous years. By using the 1997 state of the pool bottom as a reference for the computations, Figure 6b shows that scour is computed by the CFM method for average and conservative parametric assumptions on the rock mass quality.

For beneficial assumptions on the rock mass quality, computed scour formation is negligible. For average assumptions, the computed and measured scour formation as a function of flood durations are in very good agreement. This points out the adequacy of the CFM model to predict further scour formation in the plunge pool. Also, the DI method predicts ultimate scour depths that are somewhat deeper than the CFM method. This is logic because the DI model considers the ultimate state of scour.

Third, the design flood event has been applied following the 1997 event, i.e. instead of the 1998 event. As shown in Figure 6c, the computed scour formation is less restrictive than for the 1998 flood event. This at first sight rather contradictory statement can be explained by the fact that jet diffusion and energy dissipation through the pool depth before impacting the bedrock is more important for the design flood because of a higher tailwater level (193 m a.s.l. instead of 187). Hence, the corresponding maximum pressure fluctuations inside the rock joints are less.

Finally, the design flood has also been applied after the year 2000, for which a bedrock level of 125 m a.s.l. has been observed. The results are presented in Figure 6d and are very similar to the previous computations.

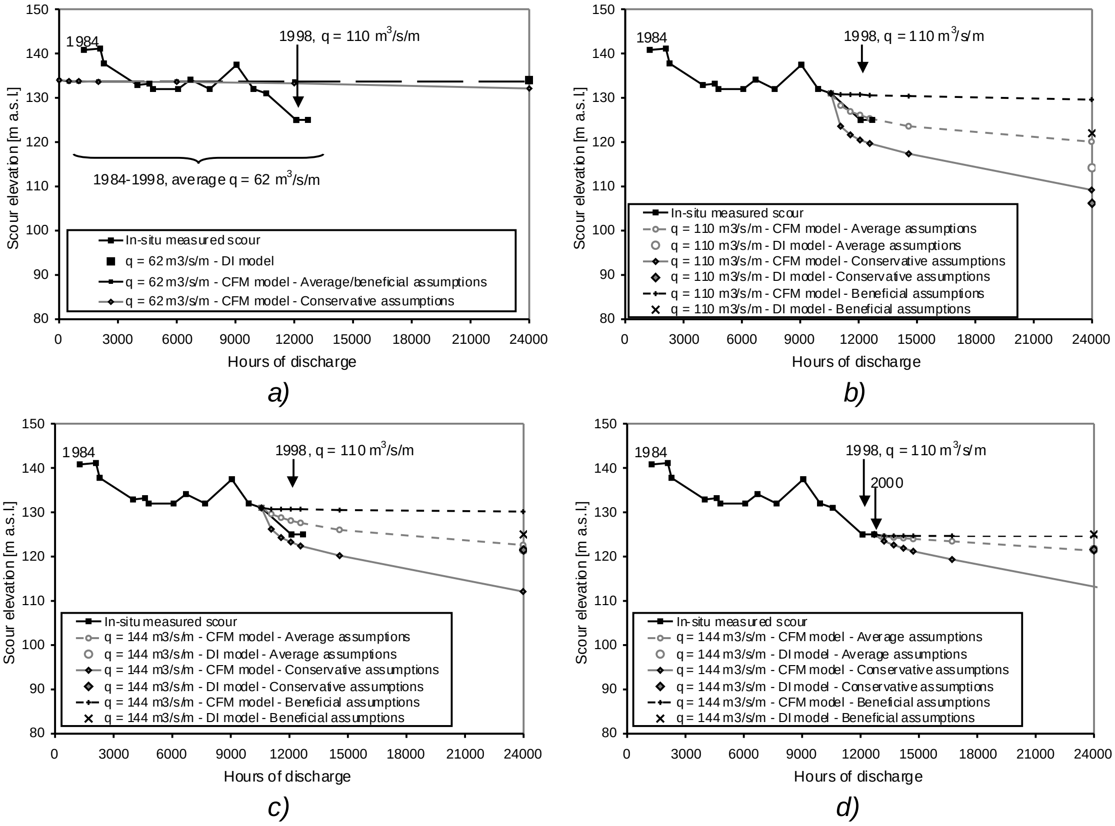

Figure 6: Results of CSM computations: a) q = 62 m²/s; b) q = 110 m²/s; c) q = 144 m²/s applied after 1998 event; d) q = 144 m²/s applied after 2000 event.

As a summary, for the 1998 flood, the CFM method predicts scour down to 126.1 m a.s.l. on the average, i.e. very close to the in-situ measured value of 125 m a.s.l. For the design flood, the CFM method predicts 124.0 m a.s.l. on the average. No in-situ measurements are available for this flood.

5. Conclusions

20 years of scour survey in the plunge pool downstream of Srisailam Dam, Andha Pradesh, India, has been used to apply the Comprehensive Scour Model (CSM) developed by Bollaert (2004). The Comprehensive Scour Model evaluates the ultimate scour depth and the scour evolution in any type of jointed rock. The model is based on near-prototype measurements of pressure fluctuations at pool bottoms and inside artificially created rock joints. It represents a comprehensive assessment of instantaneous and time-dependent (CFM method) fracturing of rock joints and of dynamic uplift (DI method) of so formed rock blocks. The CFM method is able to predict the time evolution of scour formation.

The present application shows the promising and comprehensive character of the model. Especially when past scour information is available, or when the main rock and hydraulic characteristics at the site are known, the model is able to predict future scour formation as a function of time. Its physical nature makes it also applicable to closely related engineering domains, such as uplift and/or cracking of concrete slabs of stilling slabs, or break-up of fractured coastal structures by violent wave impact.

References

1. Atkinson, B.K. (1987), "Fracture Mechanics of Rock." *Academic Press Inc.*, London.
2. Bollaert, E.F.R. (2002), "Transient water pressures in joints and formation of scour due to high-velocity jet impact." *Communication 13*, Laboratory of Hydraulic Constructions, Lausanne, Switzerland.
3. Bollaert, E.F.R. (2004), "A comprehensive model to evaluate scour formation in plunge pools." *Int. J. Hydropower & Dams*, 2004, 2004(1), pp. 94-101.
4. Bollaert, E.F.R. (2005), "The influence of geomechanic and hydrologic uncertainties on scour at large dams: case study of Kariba Dam, 73rd Annual ICOLD Meeting, Tehran, Iran.
5. Bollaert, E.F.R. and Schleiss, A.J. (2005), "A physically-based model for evaluation of rock scour due to high-velocity jet impact", *Journal of Hydraulic Engineering*, March 2005.
6. Gowda et al. (1999), "Seismic survey for detecting scour depths downstream of the Srisailam Dam", Engineering Geology, Vol. 53.
7. Mason P.J. (2000), "Sriailam Dam: A Review of downstream plunge pool development", BBV, UK.
8. Swamy, M.L. (1979), "Foundation treatment of Srisailam Dam, Water Power and Dam Construction.